Received: 14 July 2017 | Revised: 22 August 2017 | Accepted: 9 October 2017

DOI: 10.1002/pip.2954

WILEY PROGRESS IN PHOTOVOLTAICS

EU PVSEC PAPER

Understanding the light-induced degradation at elevated temperatures: Similarities between multicrystalline and floatzone p-type silicon

Tim Niewelt[1,2] | Florian Schindler[1,2] | Wolfram Kwapil[1,2] | Rebekka Eberle[1] | Jonas Schön[1,2] | Martin C. Schubert[1]

[1] Fraunhofer Institute for Solar Energy Systems ISE, Freiburg, Germany

[2] Freiburg Materials Research Centre FMF, Freiburg, Germany

Correspondence
Tim Niewelt, Fraunhofer Institute for Solar Energy Systems ISE, Freiburg, Germany.
Email: tim.niewelt@ise.fraunhofer.de

Funding information
German Federal Ministry for Economic Affairs and Energy (BMWi), Grant/Award Number: 0325763A

Abstract

This paper discusses degradation phenomena in crystalline silicon. We present new investigations of the light- and elevated temperature-induced degradation of multicrystalline silicon. The investigations provide insights into the defect parameters as well as the diffusivity and solubility of impurity species contributing to the defect. We discuss possible defect precursor species and can rule out several metallic impurities. We find that an involvement of hydrogen in the defect could explain the characteristic observations for light- and elevated temperature-induced degradation. Furthermore, we demonstrate analogies to the light-induced degradation mechanisms at elevated temperatures observed in floatzone silicon, where several experimental results also indicate an involvement of hydrogen in the defect. Based on the similarities between multicrystalline and floatzone silicon, we suggest that both degradation phenomena might be caused by the same or similar defects. As we do not expect large concentrations of metals in floatzone silicon, we suggest that complexes of hydrogen and a species introduced during crystal growth might cause both degradation phenomena.

1 | INTRODUCTION

Light-induced degradation (LID) in silicon material has been subject to extensive research efforts for several decades. The most prominent example of LID is the degradation due to the activation of boron-oxygen (BO) defects in Czochralski-grown (Cz) silicon addressed to as BO degradation or BO-LID[1,2] (and references therein). More recently, silicon with copper contamination was also shown to cause a significant lifetime decrease under illumination referred to as Cu-LID[3] (and references therein). Furthermore, the light-induced dissociation of iron-boron (or other Fe acceptor) pairs in contaminated material (e.g., Zoth and Bergholz[4] and Geerligs and Macdonald[5]) is often mentioned in the context of LID. These phenomena have a common behavior in that they can be observed upon illumination at room temperature and that the crucial components of the defects have been identified.

In 2012, Ramspeck et al extended the investigation of multicrystalline (mc) silicon passivated emitter rear contact solar cells to conditions relevant for photovoltaic module operation in the field, i.e., to illumination at elevated temperatures above ~60°C for long time scales.[6] As a result, they observed a severe drop in the cell efficiency that exceeded effects that could reasonably be explained with iron contamination or BO defects. The effect was termed light- and elevated temperature-induced degradation (LeTID) later on.[7] Several distinct differences such as the degradation kinetics, its injection dependence, and the absence of direct correlation to the concentrations of boron or interstitial oxygen indicate that LeTID is not related to BO degradation, FeB dissociation, or Cu-LID, e.g., Ramspeck et al, Fertig et al, and Vahlman et al.[6,8,9]

In the recent months and years, many different experimental observations concerning LeTID by several groups have been published, which—in conjunction—yield a set of clues that may eventually help to identify the responsible "LeTID defect". This contribution merges results from literature and findings of the authors and discusses the possible conclusions that can be drawn. Section 2 focuses on the mc materials usually associated with LeTID, while section 3 discusses implications of similar observations on monocrystalline silicon. Finally, we present a hypothesis for defect components and complex formation mechanisms underlying LeTID, which explains the degradation mechanisms in multi- and monocrystalline silicon.

2 | MULTICRYSTALLINE SILICON

2.1 | Experimental insights

The LeTID effect has been investigated by several groups on various different sample types (including different solar cell concepts) and under different conditions. After initial suggestions that the degradation might arise from the degradation of dielectric surface passivation layers,[8] many results indicate that the degradation arises from a recombination-active bulk defect.[7,10,11] The studies suggest a great variety of features of the responsible defect and factors influencing the degradation. Some of the findings recur in different studies and from different aspects, while others arise from specific experimental details. For the sake of clarity, we structure the discussion of the factors influencing the LeTID effect and features of the underlying defects into 3 parts. The first part introduces general features of the overall degradation effect and how they are affected by sample processing conditions. The observed transitions between the metastable defect states are discussed in the second part, and the third part discusses characteristic features observed in the degraded state.

2.1.1 | General features and influence of processing conditions

There are indications that different silicon materials (e.g., wafers from different mc silicon ingots or different positions in the ingot) show a different degradation behavior, e.g., Nakayashiki et al[10] and Zuschlag et al.[12] Notably, it was perceived early on that both B- and Ga-doped materials are susceptible to LeTID,[6] although there are indications that the degradation is slowed in Ga-doped material.[13] A detailed analysis of the underlying differences of the materials could provide interesting insights into the responsible defects. However, comparability of experiments on different materials from multiple studies is hindered by the observation that even the same starting material already features very different LeTID effects for slight variations in sample processing schemes, e.g., Eberle et al.[14]

In particular, the severity of LeTID seems to be determined by high-temperature applications such as the fast firing step. As Bredemeier et al,[15] Nakayashiki et al,[10] and Chan et al[16] showed, the magnitude of LeTID scales with the peak firing temperature: stronger degradation is observed at higher peak temperature. Below a threshold sample temperature of around ~700°C, no significant LeTID is observed. Besides the influence of peak temperature, an influence of the temperature ramps is observed. We demonstrated[14] that LeTID can be effectively suppressed by applying slower temperature ramps. It is still unclear whether the slower heating or cooling or the longer time above a critical temperature causes the suppression. Alternatively, the degradation behavior, i.e., the magnitude and the kinetics, can be influenced by adding a subsequent temperature treatment after the firing,[16,17] which may even lead to a suppression of the degradation effect.

In addition to the firing process, the surface passivation layer seems to have a crucial impact on LeTID: if no passivating layer is present during the firing step, no LeTID is observed.[18] The presence of dielectric passivation layers (such as silicon nitride SiN_x aluminum oxide AlO_x[18] or silicon oxide SiO_x[19]) during firing gives rise to LeTID. However, the passivation scheme affects LeTID: while SiN_x and AlO_x/SiN_x-stacks processed under identical conditions lead to a very similar behavior, samples featuring only AlO_x passivation layers show a slower and less pronounced degradation.[18]

2.1.2 | Defect state transitions

The detrimental aspect of LeTID from a solar cell perspective is the degradation of charge carrier lifetime during illumination at elevated temperature, i.e., during the typical working conditions of photovoltaic modules. The experiments of Ramspeck et al were performed at about 75°C.[6] At such temperatures, the degradation is observed on time scales of several hundred hours of illumination; i.e., it proceeds rather slowly in comparison with other LID effects. Not surprisingly, the degradation can be significantly accelerated by using higher temperatures, as shown, e.g., by Bredemeier et al who determined the activation energy of the degradation process to be ~0.9 eV.[20] Below a threshold of around 50°C, hardly any degradation is observed.[13]

The degradation is caused by illumination but also occurs under current injection, e.g., Kersten et al.[7] Thus, it is likely caused rather by excess charge carrier injection than light itself. In a recent publication, we have used this feature to create defined injection conditions in solar cells susceptible to LeTID and study the defect activation kinetics.[21] We found a linear dependence of the degradation rate constant to the injected charge carrier density Δn at least in the regime of 10^{13} to 10^{15} charge carriers per cm^3. This finding is in accordance with the observation of several groups that increased illumination intensity gives rise to a faster degradation, e.g., Payne et al.[22] So far, no saturation of the degradation rate for stronger illumination was reported, and in the study underlying Kwapil et al, we observed no saturation for strong current injection.[21] It should be noted that the investigation of the defect state transitions is hindered by their simultaneous occurrence, e.g., the likely superposition of degradation and recovery during illumination at elevated temperature.

A characteristic feature of LeTID is that the highly recombination-active degraded state of the underlying defect is metastable under the conditions that cause degradation. If the degradation conditions (i.e., charge carrier injection *and* elevated temperature) are maintained for a longer time, lifetime recovery (or regeneration) sets in. The recovery usually saturates at approximately the initial lifetime level.[23] Like the degradation, the recovery kinetics are strongly influenced by the injection conditions and temperature.[22] So far, experimental studies indicate that the resulting state is then stable to further illumination at elevated temperature, e.g., Kersten et al.[7]

This defect state is not the only state of the defect that can be reached from the degraded state. If the sample is subjected to elevated temperature without carrier injection, a lifetime recovery can be observed as well, but the resulting state is prone to redegradation upon subsequent degradation conditions. The process is usually addressed to as the annealing transition. We have observed this annealing transition at a temperature of 200°C. To our knowledge, no detailed study on its temperature dependency has been published yet. Alternatively, a similar transition to an unstable recovered state can be achieved via illumination at low temperatures (i.e., below the apparent degradation threshold temperature of 50°C), e.g., Kersten

et al.[18] This transition is carrier-driven: by applying a constant forward bias to solar cells in the dark at a temperature of ~25°C, we observed a recovery to roughly the initial solar cell parameter level (not shown here), which could be redegraded. At present, it is unclear whether the defect configurations are the same after dark anneal and carrier injection at room temperature.

There are indications that the second degradation after a defect anneal proceeds faster than the first.[24] This finding could be related to results published by Chan et al: they showed that a dark anneal of several minutes to hours can also affect the defect, if it is performed prior to degradation.[25] They demonstrated that moderate temperature annealing significantly changes the subsequent degradation: annealing between ~150°C and ~200°C accelerates the degradation, whereas annealing performed between ~225°C and ~275°C causes a slower degradation. In a later work, Chen et al[26] proved that even annealing in the dark at 175°C induces degradation followed by regeneration, which they attributed to the thermally generated minority carriers. Interestingly, as mentioned above, a (short) anneal at temperature exceeding 275°C prior to degradation can suppress the degradation.[16]

2.1.3 | Degraded state

In the degraded state, the defects responsible for LeTID introduce a strong recombination activity. It is a reasonable assumption that the recombination causing the lifetime degradation is a measure for the concentration of defects in this state. This allows investigating the spatial distribution of the LeTID defect via spatially resolved measurement techniques such as electroluminescence (EL) or photoluminescence (PL) imaging or light beam-induced current (LBIC). Such investigations have indicated that the LeTID defect is distributed in a mostly homogeneous pattern across mc silicon samples and solar cells.

Denuded zones

In the state of minimum lifetime (i.e., maximum concentration of active defects), thin regions of decreased degradation around grain boundaries have been observed, e.g., Luka et al.[24]

These regions are addressed to as denuded zones. One possible origin of these denuded zones is a kinetic effect due to the lower injection level close to grain boundaries. It could cause a local retardation of the degradation and thereby an *apparently lower* concentration at the moment of the overall degradation maximum. This source of doubt can be discarded from the investigations performed on solar cells. There, the recombination activity of grain boundaries is counteracted by compensating currents through the emitter and metal grid. Thus, the experiments we performed to study the degradation kinetics (see Kwapil et al[21]) were performed with laterally almost homogeneous injection density. We still observed typical denuded zone patterns around grain boundaries in the electroluminescence monitoring (see an example in Figure 1) and did not observe the grain boundaries to exhibit a retarded degradation. It should be noted that the same argumentation is true for LBIC studies of degraded solar cells (e.g., Luka et al[24]), which are, however, prone to effects arising from the different injection dependence in initial and degraded state.

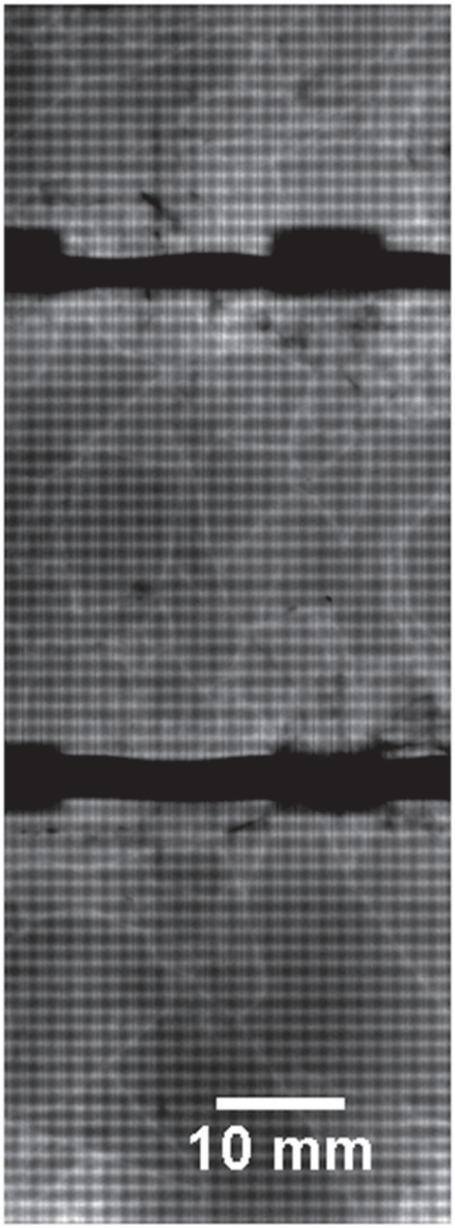

FIGURE 1 Fraction of an electroluminescence image of a passivated emitter rear contact (PERC) solar cell (p-type 1 Ωcm base material, processed for maximum LETID, see Kwapil et al[21]) at the state of maximum degradation showing denuded zones around grain boundaries. Please note that the horizontal lines of higher EL intensity arise from the local rear contacts

A second explanation for the observation of denuded zones arises from artifacts due to the strong injection dependence of charge carrier lifetime in mc silicon: for instance, a determination of the effective defect concentration $N_t^* = 1/\tau_{deg} - 1/\tau_{initial}$ from lifetime τ calibrated images featuring different excess charge carrier concentrations (with respect to time or spatial position) would implicate large errors on the derived effective defect concentration including lateral variations that might appear as denuded zones. To exclude such artifacts, we performed further studies that prove the existence of actual denuded zones of lower LeTID defect concentration: in a detailed investigation, we ensured that the initial and degraded states are evaluated at the same injection level Δn (here: $1 \cdot 10^{13}$ cm^{-3}) for every pixel. This was

achieved via interpolation of injection-dependent lifetime-calibrated PL image stacks[27] to create images at fixed injection (as discussed, e.g., in Selinger et al[28]). Beforehand, the PL lifetime images were corrected for lateral charge carrier diffusion by applying a desmearing algorithm, as suggested by Phang et al,[29] to obtain images of the real local charge carrier lifetimes. This was found to be especially important in the initial state, where high lifetimes in the grains and low lifetimes at the grain boundaries give rise to lateral current flows concealing the actual recombination mechanisms. We expect a slight remaining overestimation of N_t^* in our evaluation in regions of strong recombination (e.g., dislocation clusters) due to effects of optical blurring that affects the initial state stronger than the degraded state. The investigations confirmed that thin regions around the grain boundaries in the investigated lifetime samples feature a smaller degradation (corresponding to smaller effective defect concentrations N_t^*) than the grains themselves, which exhibit homogeneous degradation. Figure 2 exemplarily shows 3 images of a commercial 1 Ωcm p-type high-performance mc-Si wafer from these investigations: two desmeared bulk lifetime images in the initial (a) and the degraded state (b) (taken at an illumination intensity corresponding to ~1 sun) as well as an image of the effective defect concentration N_t^* (c). The denuded zones are visible both in the lifetime image in the degraded state (b) as brighter regions of increased lifetime and in the N_t^* image (c) as dark regions of reduced defect concentration. To determine the width of the denuded zones, we performed high-resolution microscopic PL investigations by using a scanning confocal microscope, as discussed in Heinz et al.[30] The total width (i.e., in both directions from the grain boundary) of the denuded zones was found to vary in a range of 200 to 400 µm. From this information, we can draw conclusions regarding the defect species responsible for LeTID, which will be discussed in section 2.2.

Defect parameters

As discussed, e.g., in Mundt et al,[31] the Shockley-Read-Hall parameters describing the recombination activity of a defect can serve as a fingerprint for its identification. Several groups have performed analyses of injection-dependent lifetime measurements to isolate the dominant defect in LeTID-affected samples and study its recombination activity.[10,32-34] As discussed in detail in Rein,[35] such investigations can determine possible pairs of the capture constant ratio k and the energy level in the band gap E_t but need further input to determine the right pair. This information can usually be derived from temperature-dependent measurements of the recombination activity of the defect. However, such investigations require the defect to remain unchanged during the measurements, which is complicated for the LeTID defect due to its strong sensitivity to temperature treatments. Therefore, most studies use the assumption that E_t is at or around the middle of the band gap, where the $k(E_t)$ function usually features a plateau. Thus, Nakayashiki et al[10] reported a value for k = 28.5, Bredemeier et al[32] determined a value for $k = 20 \pm 7$, and Morishige et al[33] reported on values in the range of $26 < k < 36$.

More recently, Vargas et al performed temperature-dependent analyses and reported ranges of k and E_t.[34] To avoid changes of the defect during the measurements, they restricted the investigated temperature range to between −25°C and 75°C. They report on two possible defect energy levels of $E_t - E_i = -(0.32 \pm 0.05)$ eV or $E_t - E_i = (0.21 \pm 0.05)$ eV in the lower and upper halves of the bandgap with corresponding values for the capture cross section ratios of $k = 56 \pm 23$ or $k = 49 \pm 21$, respectively.

All literature results reported above were obtained by making use of global measurement techniques that measure average lifetimes

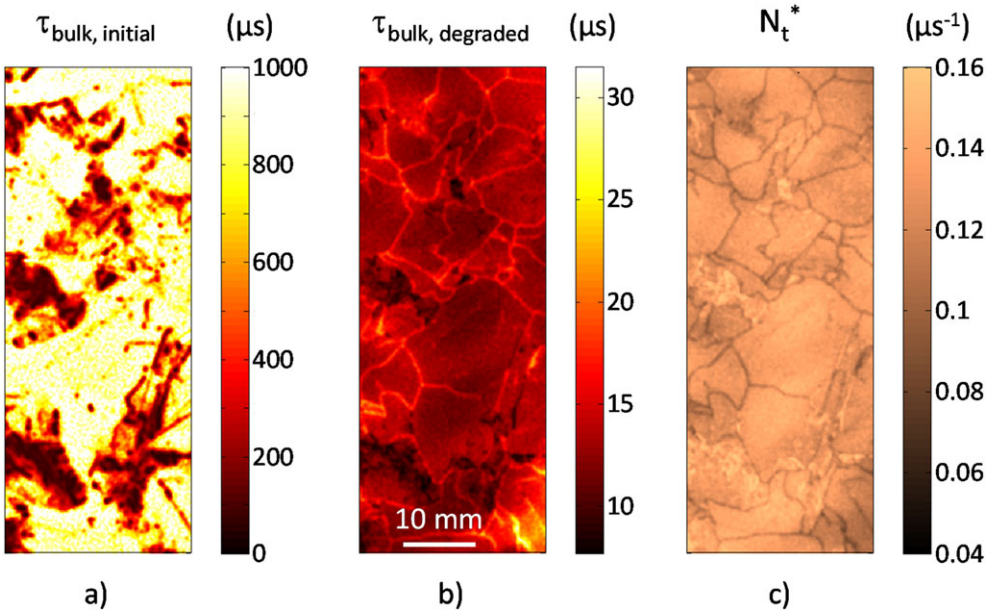

FIGURE 2 Degradation of a commercial 1 Ωcm p-type (boron doping) high-performance mc-Si wafer: (a) fraction of a lifetime-calibrated photoluminescence (PL) image taken at 1 sun equivalent in the initial state, (b) lifetime-calibrated PL image taken at 1 sun equivalent at maximum degradation after 105 hours (same sample fraction), and (c) effective defect concentration N_t^* illustrating the additional recombination caused by light- and elevated temperature-induced degradation (LeTID) defects evaluated at fixed injection level of $\Delta n = 1 \cdot 10^{13}$ cm^{-3} (same sample fraction) [Colour figure can be viewed at wileyonlinelibrary.com]

across several grains of the mc silicon. These measurements are thus affected by influences of lateral sample inhomogeneity (e.g., grain boundaries and dislocation clusters) that can affect the measured injection dependence. We performed an experiment to ensure that this experimental limitation does not cause structural misinterpretations. Based on our spatially resolved measurements, we were able to avoid the averaging over structural defects. We thereby performed an injection-dependent lifetime spectroscopy within a single grain on a wafer. The PL image stacks were corrected for lateral carrier diffusion as indicated above, and the lifetime was averaged over a homogeneous grain to reduce signal noise. Figure 3A shows the diffusion-corrected lifetime measured and averaged in a single grain of a commercial 1 Ωcm p-type high-performance mc silicon wafer (same sample as shown in Figure 2) before and after degradation (~1 sun equivalent halogen lamp illumination at ~75°C sample temperature). The recombination introduced by LeTID defects was isolated via comparison of degraded and annealed state. The quantity $\tau_{defect} = (1/\tau_{degraded} - 1/\tau_{initial})^{-1}$ was investigated as a function of the ratio of minority and majority carrier density n/p (according to the linearized SRH approach suggested by Murphy et al[36]). Thereby, we identified a dominant defect that features a ratio of capture cross sections of $k \approx 35$ (cf. Figure 3B) under the assumption of a deep defect level. We thus observe a comparable injection level dependence as that reported in literature. Therefore, we can exclude severe influences of averaging artifacts.

2.2 | Implications for the responsible defect

The various experimental findings allow narrowing down potential components of the defect complex responsible for LeTID. In the initial state of samples after typical solar cell (or lifetime sample) processing steps, little recombination activity due to LeTID defects is observed. Thus, the defect is not (or only weakly) recombination-active, indicating that most defects are either in an inactive state or not yet formed. However, as discussed above, details of the sample process greatly influence the amount and the kinetic behavior of LeTID. This indicates that they affect the concentration of formed defects or the concentration of available precursor species necessary to form the defect during a degradation treatment.

We have demonstrated in the previous section that spatially resolved investigations show denuded zones around grain boundaries. This indicates that the defect or an important precursor species is internally gettered in the grain boundaries. This internal gettering can occur either during crystallization, phosphorus diffusion, or during the cooling after the final firing step. The binding energies between crystal defects and impurities are too small to cause segregation at high temperatures.[37] Thus, the responsible gettering mechanism is most likely precipitation, which would allow gettering only at temperatures with a supersaturated impurity. Some of the impurity species observed in mc silicon can be ruled out from causing the denuded zones in LeTID as they have too low diffusivities to form denuded zones of >100 µm width. These are elements such as B, Ga, P, W, Ti, V, O_i, Zn, and Na, as they cannot diffuse far enough during typical crystal growth or any high-temperature step during the solar cell processing. Thus, the observation of denuded zones shows that they cannot be the LeTID defect by themselves but would need to form a complex with a more mobile species. This conclusion contradicts the suggestions of Nakayashiki et al and Morishige et al based on their recombination activity analyses, which suggest that the LeTID defect might be interstitial titanium (Ti_i) or substitutional tungsten (W_s).[10,33]

The assumption that the denuded zones are created during crystal growth would rule out further species, as well. Impurities that are known to diffuse fast at moderate temperatures would be redistributed homogeneously during solar cell processing (e.g., during phosphorus diffusion steps) due to a solubility below typical impurity concentrations at process temperatures. Denuded zones in solar cells and fully processed lifetime samples could therefore not have been formed by Cr, Mn, Mo, Fe, Cu, Ni, and Co during the crystallization step.

Thus, the creation of the denuded zones related to LeTID is likely to occur during the firing steps, which is in good agreement with the observation of the strong influence of the firing step process details on the LeTID defect or its precursors. If we assume that the denuded zones are formed during the cool down in the firing process, the fast-diffusing species ruled out above become the likely candidates

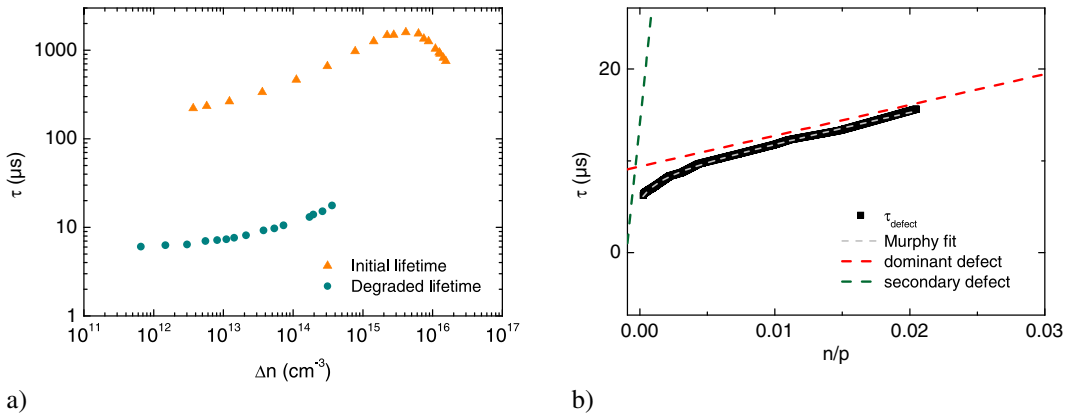

FIGURE 3 Lifetime spectroscopy in a single grain of the sample shown in Figure 2 (commercial 1 Ωcm p-type high-performance mc-Si wafer). (A) Lifetime as a function of excess carrier density before (orange triangles) and after (cyan circles) activation of light- and elevated temperature-induced degradation (LeTID) defects (~1 sun equivalent, ~75°C). (B) The defect-related lifetime limitation τ_{defect} as a function of the ratio of minority and majority carrier density $X = n/p$. The dashed lines indicate that τ_{defect} can be described by superposition of 2 defects. The dominant defect features a value of $k \approx 35$ assuming a midband energy level [Colour figure can be viewed at wileyonlinelibrary.com]

for defect precursors. However, for the typical times and temperatures of firing processes, even the diffusivities of Cr, Mn, Mo, and Fe are too small to explain the width of the denuded zones. This leaves Cu, Ni, and Co as possible candidates featuring diffusivities in a suitable range (e.g., Graff[38]) to form denuded zones of >100 μm width during cooling down. One of these elements, Cu, has already been shown to cause LID. However, several features of Cu-LID differ significantly from LeTID; e.g., (i) Cu-LID occurs also at room temperature[3] as opposed to an apparent onset of LeTID at elevated temperature, (ii) Cu-LID proceeds significantly faster than LeTID,[9] and (iii) the capture cross section ratio k of the dominant defect in the degraded state has been determined to 1.7 to 2.6[39] compared with k~30 for LeTID. In addition, no observation of a regeneration comparable with the complete LeTID cycle has been reported so far. Therefore, we exclude the possibility that Cu-LID and LeTID are identical phenomena, although a participation of Cu in LeTID cannot be dismissed in this line of argument. Yet, both copper and nickel are unlikely candidates for a different reason: the solubility of Cu is, similar to Ni, quite high, and all Cu complexes should dissolve already at temperatures well below typical T_{peak} of the firing process. In that case, the strong dependency of the LeTID on T_{peak} cannot be explained.

In contrast, in the interesting peak temperature range, the solubility of Co rises from $S_{Co} \approx 2 \times 10^{11}$ cm^{-3} at 700°C to $S_{Co} \approx 1 \times 10^{12}$ cm^{-3} at 750°C, which is in the range of typical Co concentrations in as-grown mc silicon originating from crucible coatings.[40,41] For lower temperatures, the solubility of Co strongly declines (e.g., $S_{Co} \approx 5 \times 10^{9}$ cm^{-3} at 600°C), which could explain the sensitivity of LeTID to the firing step peak temperature. During typical phosphorus diffusion gettering processes, the total Co concentration decreases by around two orders of magnitude,[41] which is in agreement with the observation of reduced LeTID in gettered samples.[12] Together with its suitable diffusivity, this renders cobalt the most interesting candidate from the typical metal impurities for being involved in LeTID.

Additionally, a variety of different Co defects are known.[38,42] As mentioned above, the extent of LeTID degradation clearly correlates with the temperature ramps of the firing process.[14] In this context, the reported sensitivity of Co to cooling rates after high temperature steps is remarkable: while slow cooling processes lead to a diffusion of Co to the wafer surface, fast cooling ramps can facilitate its agglomeration in precipitates in the volume.[38] It should be noted that these forms of Co were observed in intentionally contaminated monocrystalline silicon and that further species might exist in mc silicon due to the presence of additional nucleation sites. Interesting candidates for the LeTID defect in the variety of known Co-related defects are the complexes of Co and hydrogen, which are believed to be recombination-active.[38]

Hydrogen is also a likely candidate for a precursor species by itself. While not a common species in freshly crystallized material, it is well known to be introduced to silicon from the wafer surfaces during firing steps, especially in the presence of hydrogen-rich dielectric passivation layers. The diffusivity of hydrogen depends very much on the specific sample and process conditions (e.g., Sun et al[43]) but is high enough to penetrate to the wafer bulk. The large density of defects (e.g., dangling bonds) at grain boundaries makes them effective sinks for H, potentially creating hydrogen-denuded zones.

3 | MONOCRYSTALLINE SILICON

It has been demonstrated recently that LeTID also occurs on monocrystalline p-type Cz silicon.[26,44] The effect is observed in addition to the conventional BO degradation or after specific process steps to mitigate BO defect activation. This finding supports the idea that LID effects observed in floatzone (FZ) silicon (e.g., by Sperber et al[45,46] and Niewelt et al[47]) might arise from a similar or the same defect. We had suggested this possibility in Niewelt et al[47] but now regard it as even more likely in the light of the reports on LeTID in Cz silicon. In the first part of this section, we therefore report the experimental findings on FZ-LID that bear similarity to LeTID. For the sake of brevity, our own experimental results on FZ-LID are only mentioned in summarized form in the same structure as used in section 2.1. For further details, please refer to Niewelt et al.[47] The second part discusses the observed effects and potential implications for LeTID.

3.1 | Similarities of floatzone-LID and light- and elevated temperature-induced degradation

3.1.1 | General features and influence of processing conditions

An important similarity of LeTID and FZ-LID is that significant degradation is only observed on p-type samples after passivation with dielectric layers and subjection to a short high temperature step ("firing"). We did not observe FZ-LID on n-type samples and are not aware of reported LeTID on n-type material. The peak temperature of the firing step T_{peak} was observed to have a strong impact on the magnitude of the FZ-LID effect. The effect ranged from slight lifetime reduction for moderate T_{peak} around 700°C to a severe τ_{eff} decay for T_{peak} of 900°C, measured on equally processed samples. No clear degradation was observed for sister samples fired at only 650°C or subjected to slow-rate annealing steps at 425 to 450°C. It should be noted that we observed FZ-LID, although our samples were fired with rather slow cooling ramps (in fact, the exact same firing processes that caused only weak LeTID in our study presented in Eberle et al[14]). Besides the dependence on the firing step, we observe a crucial influence of SiN_x capping layers: significant degradation was only observed when a SiN_x layer was present, either as a single film (see Sperber et al[45]) or on top of the AlO_x layers that we used to passivate our samples. By contrast, at the same T_{peak} of 800°C, the omission of SiN_x capping layers drastically reduced the degradation effect.

3.1.2 | Defect state transitions

Besides these similar preconditions of the sample processing, there are parallels concerning the observed defect state transitions. We observed the FZ-LID under the same conditions as applied in many studies of LeTID, i.e., ~1 sun equivalent halogen lamp illumination at ~75°C sample temperature. Sperber et al also demonstrated the effect to occur at higher temperatures.[46] By dark annealing FZ samples, degraded state can be reverted to a high lifetime state that is prone to repeated degradation,[45] resembling the effect of annealing of LeTID defects. We also observed a lifetime recovery of degraded FZ samples upon illumination at room temperature with a laser, resembling the light-induced annealing of LeTID defects.

When the conditions that cause degradation (i.e., illumination at elevated temperature) were maintained after complete degradation, samples affected by FZ-LID exhibited a complete lifetime recovery. The resulting state was demonstrated to be stable to further exposition to degradation conditions, as demonstrated in Niewelt et al.[48] In summary, our experiments demonstrate that the same transitions observed in samples affected by LeTID occur in samples prone to FZ-LID. However, the processes occurred on different—i.e., significantly shorter—time scales in the FZ samples. Under the tested degradation conditions, the whole cycle of degradation and complete recovery was completed in less than 40 hours compared with typically several hundred hours for LeTID.

3.1.3 | Degraded state

In our study of FZ-LID, we applied PL imaging to investigate the lateral distribution of the effect. In the FZ-LID degraded state, the wafers featured a characteristic ring pattern. We observed fine striations in the measured PL intensity in a range of 5%. An example is given in Figure 4 for an FZ sample featuring in degraded state. These local variations are likely to be associated with a lateral variation of the concentration of the defect causing FZ-LID. Similar patterns have been shown for the variation of the doping concentration of FZ wafers, e.g., by Lim et al.[49] Thus, it appears that the defect responsible for FZ-LID includes either dopant atoms or a yet unknown species, which is distributed alike during the FZ crystallization process. In mc silicon, the strong lateral inhomogeneities caused by structural features and the superposition with other recombination channels make it difficult to observe or exclude such features. However, we observed a similar pattern in the lateral distribution of the degradation time constants[28] that might be related to lateral doping variations in mc ingots.

The additional recombination introduced by the bulk defects responsible for FZ-LID exhibits a strong injection dependence. We performed an analysis of the isolated defect-related lifetime limitation τ_{defect} similar to the one presented in section 2.1.3. Good agreement with the measurements was achieved under the assumption of a deep defect level with a capture cross section ratio $k \approx 30$. Sperber et al found a similar value for k of 20 ± 2.[45] In our experiments, samples prone to FZ-LID featured indications of this injection-dependent recombination already in initial state. This supports the assumption that a fraction of the defects causing FZ-LID might be present/active directly after sample processing. If this is the case, the defects observed by Grant et al[50] might be the same, which is supported by the similar value of $k \approx 26$ they found to fit their data. Note that these values reported for FZ silicon thus show good agreement with the ranges reported for LeTID, as discussed in section 2.1.3.

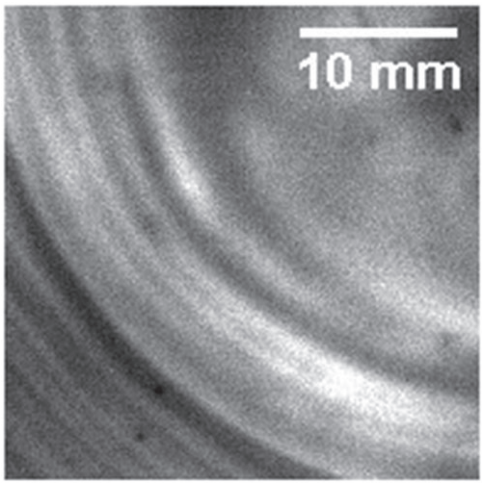

FIGURE 4 Fraction of a photoluminescence (PL) image of a p-type 1 Ωcm floatzone (FZ) sample (processed for strong FZ-LID, as discussed in Niewelt et al[47]) in FZ-LID degradation maximum

3.2 | Discussion and implications

This set of similarities is no proof that the underlying defects are actually the same. However, we consider it reasonable to discuss the potential implications concerning LeTID.

The observation of shorter process durations in the FZ samples agrees well with the concept that electrons (or more general excess charge carriers) play a role in the defect state transitions. Besides the observed influence of illumination intensity on the transitions of LeTID affected samples, this concept is supported by our study presented in Kwapil et al.[21] There, we demonstrated a direct correlation of the degradation rate constant of mc silicon-based solar cells and the injected charge carrier concentration. The FZ samples we investigated featured an excellent surface passivation and low background recombination caused by contaminations or structural defects. Therefore, the same illumination conditions gave rise to a higher excess charge carrier concentration Δn than in typical mc silicon samples, which provides a good explanation for the faster degradation and recovery. An estimation of the injection level in the FZ and mc samples during illumination supports that the degradation-recovery cycles are quite comparable, if the influence of Δn is taken into account.

Thus, the kinetics of LeTID are sensitive to lifetime limitations introduced by other defects in the material or influences of surface passivation, metal contacts, etc. For mc silicon, this implies that higher material purity and crystallographic quality affect the observed LeTID, potentially explaining several observations in literature, e.g., Kersten et al, Nakayashiki et al, and Zuschlag et al.[7,10,12] For Cz grown silicon, a strong influence of lifetime limitations induced by BO defects can be expected. Besides arising apparent influences of the concentrations of boron and interstitial oxygen, it must be kept in mind that the transitions between different BO defect states are also known to occur at the conditions used for investigation of LeTID. Similar considerations should be true for other metastable defects such as FeB and CrB pairs or Cu-LID.

The central implication of LeTID in Cz and FZ silicon concerns the question which precursor species appear to be reasonable. In section 2.2, we have discussed several potential precursor species based on the common contaminants in mc silicon and identified the most likely ones. Given that Cz and FZ silicon are grown under different conditions concerning cleanliness and growth conditions than mc silicon, different crystal defect species are expected. The incorporation of metal contaminations (including Cobalt) during crystal growth can be expected to be orders of magnitude smaller than for typical mc silicon. Thus, potential defect precursors are most likely to be

either intrinsic lattice defects such as interstitial silicon atoms Si_i or lattice vacancies V_{Si} (e.g., Falster and Voronkov[51]), the dopant species boron (or Ga), nitrogen introduced during crystal growth (e.g., Grant et al[50]), or species introduced from the wafer surfaces during processing.

As mentioned in section 2.2, the dopant species should not show denuded zones and can therefore not be the concentration-limiting precursor species.

A species that is known to be introduced to silicon wafers during the process sequences giving rise to LeTID and FZ-LID is hydrogen. An involvement of H in the defect formation could explain the influences of surface passivation layers and the firing conditions. Release of H from dielectric passivation layers during thermal treatments is expected, and peak temperatures above 600°C would allow its diffusion throughout the wafer thickness (e.g., Wilking et al, Dekkers et al, Hallam et al, and Mathiot,[52-55] and references therein). H atoms themselves are not likely to be recombination-active defects. Also, many crystal defects can be effectively passivated upon binding with hydrogen (e.g., grain boundaries[56,57]). However, formation and subsequent dissolution or evolution of a recombination-active H complex would be a valid explanation for observations related to LeTID and FZ-LID. The diffusivity of hydrogen varies by orders of magnitude depending on its charge state, which can be influenced by illumination, e.g., Sun et al and Hamer et al.[43,58] The conditions applied for degradation increase the concentration of neutral hydrogen H^0, which is very mobile and can therefore diffuse to other defect precursors. The necessity to promote recharging of hydrogen might also be the underlying mechanism causing the dependence of the degradation rate on Δn discussed in Kwapil et al.[21]

The lateral distribution of FZ-LID we have observed exhibited a characteristic striation pattern. This implies that a grown-in species in the wafers contributes to the defect causing FZ-LID. This structure could arise from slight instabilities of the FZ growth process that cause a variation of the intrinsic defect concentration. It is a reasonable assumption that the FZ and Cz samples we and the other groups have investigated were cut from crystals grown rather vacancy-rich due to throughput considerations. However, this is speculative and the inclusion of intrinsic lattice defects in mc silicon depends on the specific growth conditions. We can therefore neither confirm nor exclude the involvement of Si_i or V_{Si} but consider them interesting candidates for future investigations.

4 | CONCLUSION

In this work, we have discussed LID effects observed in mc and FZ silicon. In the first part, we excluded many typical defects from playing an important role in LeTID in mc silicon based on the occurrence of denuded zones. Species that are known to diffuse slowly are unlikely to show depletion on the length scales observed for the widths of the denuded zones. They can therefore only be precursors of the LeTID defect if they form a complex with a fast-diffusing species. Cobalt and hydrogen were identified as species that could create recombination-active defects and feature suitable diffusivities to form the observed denuded zones. Also, both species are known to be affected by fast high-temperature steps. The involvement of hydrogen would further explain the influences of dielectric passivation layers.

The second part of this paper compares features of an LID effect observed in FZ silicon samples to those of LeTID in mc silicon. We demonstrate that both effects are very similar and thus might arise from similar or even the same defect reactions. If both degradation effects are caused by the same defect, the similar extent of degradation in FZ silicon renders the involvement of metal contaminations unlikely. In this line of reasoning, LeTID is suggested to be caused by defect complexes of mobile hydrogen and an intrinsic crystal defect.

ACKNOWLEDGEMENTS

This work was supported by the German Federal Ministry for Economic Affairs and Energy (BMWi) and by the industry partners within the research cluster SolarLIFE under contract no 0325763A. The authors are responsible for the content.

ORCID

Tim Niewelt http://orcid.org/0000-0002-0360-2942
Florian Schindler http://orcid.org/0000-0001-7639-2758
Wolfram Kwapil http://orcid.org/0000-0001-8489-1805

REFERENCES

1. Bothe K, Schmidt J. Electronically activated boron-oxygen-related recombination centers in crystalline silicon. *J Appl Phys*. 2006;99:13701.
2. Niewelt T, Schön J, Warta W, Glunz SW, Schubert MC. Degradation of crystalline silicon due to boron oxygen defects. *IEEE Journal of Photovoltaics*. 2016;7:383-398.
3. Lindroos J, Savin H. Review of light-induced degradation in crystalline silicon solar cells. *Solar Energy Materials and Solar Cells*. 2016;147:115-126.
4. Zoth G, Bergholz W. A fast, preparation-free method to detect iron in silicon. *J Appl Phys*. 1990;67:6764-6771.
5. Geerligs LJ, Macdonald D. Dynamics of light-induced FeB pair dissociation in crystalline silicon. *Appl Phys Lett*. 2004;85:5227-5229
6. Ramspeck K, Zimmermann S, Nagel H, Metz A, Gassenbauer Y, Birkmann B, Seidl A. "Light induced degradation of rear passivated mc-Si solar cells", presented at the 27th EUPVSEC, Frankfurt, Germany, 2012;861-865.
7. Kersten F, Engelhart P, Ploigt H-C, et al. Degradation of multicrystalline silicon solar cells and modules after illumination at elevated temperature. *Solar Energy Materials and Solar Cells*. 2015;142:83-86.
8. Fertig F, Krauß K, Rein S. Light-induced degradation of PECVD aluminium oxide passivated silicon solar cells. *physica status solidi (RRL)—Rapid Research Letters*. 2015;9:41-46.
9. Vahlman H, Wagner M, Wolny F, et al. Light-induced degradation in quasi-monocrystalline silicon PERC solar cells: indications on involvement of copper. *physica status solidi (a)*. 2017;214:1700321.
10. Nakayashiki K, Hofstetter J, Morishige AE, et al. Engineering solutions and root-cause analysis for light-induced degradation in p-type multicrystalline silicon PERC modules. *IEEE Journal of Photovoltaics*. 2016;6:860-868.
11. Luka T, Eiternick S, Frigge S, Hagendorf C, Mehlich H, Turek M. "Investigation of light induced degradation of multi-crystalline PERC cells", presented at the 31st EUPVSEC, Hamburg, Germany, 2015:826-828. https://dx.doi.org/10.4229/EUPVSEC20152015-2BV.8.12.
12. Zuschlag A, Skorka D, Hahn G. Degradation and regeneration in mc-Si after different gettering steps. *Progress in Photovoltaics: Research and Applications*. 2017;25:545-552.

13. Fritz J, Zuschlag A, Skorka D, Schmidt A, Hahn G. "Impact of temperature and doping on LeTID and regeneration in mc-Si", presented at the 33rd EUPVSEC, Amsterdam, The Netherlands, 2017
14. Eberle R, Kwapil W, Schindler F, Schubert MC, Glunz SW. Impact of the firing temperature profile on light induced degradation of multicrystalline silicon. *physica status solidi (RRL)—Rapid Research Letters*. 2016;10:861-865.
15. Bredemeier D, Walter D, Herlufsen S, Schmidt J. Lifetime degradation and regeneration in multicrystalline silicon under illumination at elevated temperature. *Aip Advances*. 2016;6:035119. https://dx.doi.org/10.1063/1.4944839
16. Chan CE, Payne DNR, Hallam BJ, et al. Rapid stabilization of high-performance multicrystalline P-type silicon PERC cells. *IEEE Journal of Photovoltaics*. 2016;6:1473-1479.
17. Engelhart P, Kersten F. "Solarzellenherstellungsverfahren und Solarzellenbehandlungsverfahren solar cells and solar cell manufacturing processes treatment". Google Patents: Germany; 2015.
18. Kersten F, Heitmann J, Müller JW. Influence of Al2O3 and SiNx passivation layers on LeTID. *Energy Procedia*. 2016;92:828-832.
19. Skorka D, Zuschlag A, Hahn G. "Spatially resolved degradation and regeneration kinetics in mc-Si", presented at the 32nd EUPVSEC, Munich, Germany, 2016:643-646. https://dx.doi.org/10.4229/EUPVSEC20162016-2AV.1.26.
20. Bredemeier D, Walter D, Schmidt J. Light-induced lifetime degradation in high-performance multicrystalline silicon: detailed kinetics of the defect activation. *Solar Energy Materials & Solar Cells*, 2017;173:2-5.
21. Kwapil W, Niewelt T, Schubert MC. Kinetics of carrier-induced degradation at elevated temperature in multicrystalline silicon solar cells. *Solar Energy Materials & Solar Cells*, vol. (available online. 2017; https://doi.org/10.1016/j.solmat.2017.05.066
22. Payne DNR, Chan CE, Hallam BJ, et al. Rapid passivation of carrier-induced defects in p-type multi-crystalline silicon. *Solar Energy Materials and Solar Cells*. 2016;158:102-106.
23. Jensen MA, Morishige AE, Hofstetter J, Needleman DB, Buonassisi T. Evolution of LeTID defects in p-type multicrystalline silicon during degradation and regeneration. *IEEE Journal of Photovoltaics*. 2017;7:980-987.
24. Luka T, Großer S, Hagendorf C, Ramspeck K, Turek M. Intra-grain versus grain boundary degradation due to illumination and annealing behavior of multi-crystalline solar cells. *Solar Energy Materials and Solar Cells*. 2016;158:43-49.
25. Chan C, Fung TH, Abbott M, et al. Modulation of carrier-induced defect kinetics in multi-crystalline silicon PERC cells through dark annealing. *Solar RRL*. 2017;1:1600028. https://dx.doi.org/10.1002/solr.201600028
26. Chen D, Kim M, Stefani BV, et al. Evidence of an identical firing-activated carrier-induced defect in monocrystalline and multicrystalline silicon. *Solar Energy Materials & Solar Cells*. 2017;172:293-300.
27. Giesecke JA, Schubert MC, Michl B, Schindler F, Warta W. Minority carrier lifetime imaging of silicon wafers calibrated by quasi-steady-state photoluminescence. *Solar Energy Materials & Solar Cells*. 2011;95:1011-1018.
28. Selinger M, Kwapil W, Schindler F, et al. Spatially resolved analysis of light induced degradation of multicrystalline PERC solar cells. *Energy Procedia*. 2016;92:867-872.
29. Phang SP, Sio HC, Macdonald D. Carrier de-smearing of photoluminescence images on silicon wafers using the continuity equation. *Appl Phys Lett*. 2013;103:192112.
30. Heinz FD, Mundt LE, Warta W, Schubert MC. A combined transient and steady state approach for robust lifetime spectroscopy with micrometer resolution. *physica status solidi (RRL)—Rapid Research Letters*. 2015;9:697-700.
31. Mundt LE, Schubert MC, Schön J, et al. Spatially resolved impurity identification via temperature- and injection-dependent photoluminescence imaging. *IEEE Journal of Photovoltaics*. 2015;5:1503-1509.
32. Bredemeier D, Walter D, Herlufsen S, Schmidt J. Understanding the light-induced lifetime degradation and regeneration in multicrystalline silicon. *Energy Procedia*. 2016;92:773-778.
33. Morishige AE, Jensen MA, Needleman DB, et al. Lifetime spectroscopy investigation of light-induced degradation in p-type multicrystalline silicon PERC. *IEEE Journal of Photovoltaics*. 2016;6:1466-1472.
34. Vargas C, Zhu Y, Coletti G, et al. Recombination parameters of lifetime-limiting carrier-induced defects in multicrystalline silicon for solar cells. *Appl Phys Lett*. 2017;110:092106. https://dx.doi.org/10.1063/1.4977906
35. Rein S. *Lifetime Spectroscopy: A Method of Defect Characterization in Silicon for Photovoltaic Applications*. Berlin Heidelberg: Springer; 2005.
36. Murphy JD, Bothe K, Krain R, Voronkov VV, Falster RJ. Parameterisation of injection-dependent lifetime measurements in semiconductors in terms of Shockley-Read-Hall statistics: an application to oxide precipitates in silicon. *J Appl Phys*. 2012;111:113709. https://doi.org/10.1063/1.4725475
37. Seibt M, Abdelbarey D, Kveder V, et al. Interaction of metal impurities with extended defects in crystalline silicon and its implications for gettering techniques used in photovoltaics. *Materials Science and Engineering: B*. 2009;159:264-268.
38. Graff K. *Metal Impurities in Silicon-Device Fabrication, 2nd ed*. Berlin: Springer; 2000.
39. Inglese A, Lindroos J, Vahlman H, Savin H. Recombination activity of light-activated copper defects in p-type silicon studied by injection- and temperature-dependent lifetime spectroscopy. *J Appl Phys*. 2016;120:125703.
40. Schubert MC, Schon J, Schindler F, et al. Impact of impurities from crucible and coating on mc-silicon quality—the example of iron and cobalt. *IEEE Journal of Photovoltaics*. 2013;3:1250-1258.
41. Schön J, Schindler F, Kwapil W, et al. Identification of the most relevant metal impurities in mc n-type silicon for solar cells. *Solar Energy Materials and Solar Cells*. 2015;142:107-115.
42. Gibbons TM, Backlund DJ, Estreicher SK. Cobalt-related defects in silicon. *J Appl Phys*. 2017;121:045704. https://dx.doi.org/10.1063/1.4975034
43. Sun C, Rougieux FE, Macdonald D. A unified approach to modelling the charge state of monatomic hydrogen and other defects in crystalline silicon. *J Appl Phys*. 2015;117:045702. https://doi.org/10.1063/1.4906465
44. Fertig F, Lantzsch R, Mohr A, et al. Mass production of p-type Cz silicon solar cells approaching average stable conversion efficiencies of 22%. *Energy Procedia*. 2017;124:338-345.
45. Sperber D, Herguth A, Hahn G. A 3-state defect model for light-induced degradation in boron-doped float-zone silicon. *physica status solidi (RRL)—Rapid Research Letters*. 2017;11:1600408. https://doi.org/10.1002/pssr.201600408
46. Sperber D, Heilemann A, Herguth A, Hahn G. Temperature and light-induced changes in bulk and passivation quality of boron-doped float-zone silicon coated with SiN:H. *IEEE Journal of Photovoltaics*. 2017;7:463-470.
47. Niewelt T, Selinger M, Grant NE, Kwapil W, Murphy JD, Schubert MC. Light-induced activation and deactivation of bulk defects in boron-doped float-zone silicon. *J Appl Phys*. 2017;121:185702. https://doi.org/10.1063/1.4983024
48. Niewelt T, Kwapil W, Selinger M, Richter A, Schubert MC. Long-term stability of aluminium oxide based surface passivation schemes under illumination at elevated temperatures. *IEEE Journal of Photovoltaics*. 2017;7:1197-1202.
49. Lim SY, Forster M, Zhang X, et al. Applications of photoluminescence imaging to dopant and carrier concentration measurements of silicon wafers. *IEEE Journal of Photovoltaics*. 2013;3:649-655.

50. Grant NE, Rougieux FE, Macdonald D, Bullock J, Wan Y. Grown-in defects limiting the bulk lifetime of p-type float-zone silicon wafers. *J Appl Phys*. 2015;117:055711. https://doi.org/10.1063/1.4907804

51. Falster R, Voronkov VV. The engineering of intrinsic point defects in silicon wafers and crystals. *Materials Science and Engineering: B*. 2000;73:87-94.

52. Wilking S, Herguth A, Hahn G. Influence of hydrogen on the regeneration of boron-oxygen related defects in crystalline silicon. *J Appl Phys*. May 2013;113:194503. https://doi.org/10.1063/1.4804310

53. Dekkers HFW, Carnel L, Beaucarne G. Carrier trap passivation in multicrystalline Si solar cells by hydrogen from SiNx:H layers. *Appl Phys Lett*. 2006;89:013508. https://dx.doi.org/10.1063/1.2219142

54. Hallam BJ, Hamer PG, Wenham SR, et al. Advanced bulk defect passivation for silicon solar cells. *IEEE Journal of Photovoltaics*. 2014;4:88-95.

55. D. Mathiot, "Modeling of hydrogen diffusion in n-type and p-type silicon", *Physical Review B*. 1989;40:5867-5870.

56. Hallam BJ, Hamer PG, Wang SS, et al. Advanced hydrogenation of dislocation clusters and boron-oxygen defects in silicon solar cells. *Energy Procedia*. 2015;77:799-809.

57. Karzel P, Ackermann M, Gröner L, et al. Dependence of phosphorus gettering and hydrogen passivation efficacy on grain boundary type in multicrystalline silicon. *J Appl Phys*. 2013;114:244902.

58. Hamer P, Wang S, Hallam B, et al. Laser illumination for manipulation of hydrogen charge states in silicon solar cells. *physica status solidi (RRL)—Rapid Research Letters*. 2015;9:111-114.

How to cite this article: Niewelt T, Schindler F, Kwapil W, Eberle R, Schön J, Schubert MC. Understanding the light-induced degradation at elevated temperatures: Similarities between multicrystalline and floatzone p-type silicon. *Prog Photovolt Res Appl*. 2018;26:533–542. https://doi.org/10.1002/pip.2954